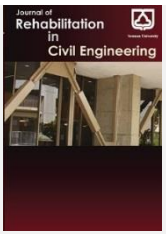

Journal of Rehabilitation in Civil Engineering

Journal homepage: https://civiljournal.semnan.ac.ir/

Comparison between Calculating Live Load Distribution Factors by AASHTO-LRFD Equations and Finite Element Method of Precast Concrete U-Girder Bridges

Kamel T. Kamel [1,*]; Ahmed H. Amer [2]; Ahmed Z. Hanafi [3]

1. Department of Civil Engineering, Obour High Institute for Engineering and Technology, Cairo, Egypt
2. Department of Civil Engineering, Elgazeera High Institute for Engineering, Cairo, Egypt
3. Department of Civil Engineering, Faculty of Engineering, Cairo University, Giza, Egypt
* Corresponding author: *dr.kameltamer@ohie.edu.eg*

ARTICLE INFO

Article history:
Received:
Revised:
Accepted:

Keywords:
Live load distribution factors;
AASHTO specifications;
Finite element analysis;
U-girder bridges.

ABSTRACT

The main objective of this study is to make a comparison between calculating live load distribution factors using AASHTO-LRFD equations and the finite element analysis of precast concrete U-girder bridges. The AASHTO-LRFD specifications provide empirical equations for calculating the distribution factors. Little information is available regarding the accuracy of these equations for this kind of bridge girder. As a result, an extensive parametric study was carried out using finite element modelling to evaluate the parameters that influence the live load distribution factors and to verify the accuracy of the AASHTO-LRFD equations to calculate these factors. The parameters considered in this study were bridge span, girder spacing, number of girders, and number of lanes. 52 prototype bridges were analysed using CSI Bridge software to determine moment and shear distribution factors due to the effect of the AASHTO-LRFD live load model (HL-93). All of the bridges studied were assumed to have straight and simply supported spans. According to the study's results, the length of the girder does not affect the LLDF, while the parameters of the distance between girders, girder count, and lane count have a significant impact. In most cases, the AASHTO equations overestimate the calculated moment and shear distribution factors. Especially for wide bridges, the parametric study found that the difference between AASHTO equations and FEA results for calculating shear distribution factors was 87%. Consequently, it is best to avoid using these equations on wide bridges.

E-ISSN: 2345-4423

How to cite this article:
Kamel, K., Amer, A., & Hanafi, A. (2024). Comparison between Calculating Live Load Distribution Factors by AASHTO-LRFD Equations and Finite Element Method of Precast Concrete U-Girder Bridges. Journal of Rehabilitation in Civil Engineering, 12(4), 103-115. https://doi.org/10.22075/jrce.2024.32025.1911

1. Introduction

Bridge safety, considered one of the most crucial parts of the infrastructure, has constantly presented significant obstacles to designers. Failures cannot be tolerated because it takes so much time and money to analyze, design, and build these bridges. Bridges are constructed to be stable and usable for the duration of their service lives. When the external environment does not change significantly, a bridge with good construction quality and materials can safely carry out its functions for the duration of its design lifetime and service life. However, over time, bridges suffer damage from several factors, including deterioration of the materials and changes in the traffic environment [1-3]. The deterioration of the materials is mainly due to the effects of long-term creep, shrinkage, and cracking of concrete [4-5]. Currently, bridge inspections and safety diagnoses are routinely performed, and bridge load-carrying capacity is assessed to determine the level of deterioration and performance degradation [6-8]. Overall, a vehicle-loading test is carried out to determine a bridge's load-carrying capacity [9-11]. Mostly, vehicle-loading tests are performed to measure the field deflections, which, in turn, are indicators to determine the safety conditions of the bridge [12-13]. A bridge's intersection and balanced performance are easily determined by calculating live load distribution factors with a vehicle-loading test. When a load is applied to a girder, the load is shared by the adjacent girders. In this situation, the level of load transmission is determined by the rigidity of the girders and the distance between the girders. Therefore, LLDF is a significant factor in bridge design or maintenance [14-16]. Calculating the straining actions of a bridge girder under loads of service accurately might be a challenging assignment because the straining actions of a bridge girder depend on several factors, including the load position, bridge type, girder spacing, and span length [17-18].

In this study, AASHTO's LRFD Bridge Design Specifications were used [19]. The live load model of AASHTO-LRFD provided various formulas to make calculating the live load effect on bridges simple and easy. The truckload and distributed loads are used to indicate the actual live load, which may be mixed and positioned to simulate the impact of the actual live load. To get the best impact on bridge elements, the designer should distribute the truckload and distribute load longitudinally through the bridge span and laterally through the bridge deck.

The usage of precast U-girders is now gaining popularity. Additionally, precast U-Girder bridges have the advantages of being economical, extremely stiff, and requiring little internal bracing [20-21]. While U-girders are becoming more common, questions have arisen about the design of bridges using this girder type. Because the precast U-girder is a new girder type, there is little information available on how it will behave as the bridge ages. As a result, this research was conducted to investigate the behavior of precast U-girder bridges and calculate the live load distribution factors to be used in the design.

CSI Bridge Software was used to analyse the studied bridges using three-dimensional finite elements. The CSI Bridge software is an advanced version of SAP 2000 software that is multifaceted programming software specifically created for bridges [22-23]. Influence parameters considered in this study were bridge span, girder spacing, the number of girders, and the number of lanes. For each of these parameters, the distribution factors from the finite element models and AASHTO-LRFD equations were calculated for multi-lane loading.

The AASHTO-LRFD specifications provide empirical equations for calculating the distribution factors. Little information is available regarding the accuracy of these equations for this kind of bridge girder.

Therefore, the main objective of this research is to make a comparison between calculating live load distribution factors using AASHTO-LRFD equations and the finite element analysis of precast concrete U-girder bridges. The objective of this comparison is to examine the level of accuracy of the AASHTO-LRFD equations.

2. Background

There have been no studies to evaluate LLDF on precast concrete U-girder bridges, but some studies have been conducted to evaluate LLDF for other bridges [24-27]. The researchers found that LLDF is affected by several parameters, including girder location, lane count, distance between girders, and girder length. Spacing between girders is regarded as an important parameter influencing load distribution factors. According to AASHTO Standard Specifications, spacing between girders is the sole factor that influences lateral load distribution. As a result, the standard specifications assume that the load distribution factors and girder spacing between girders have a linear correlation. However, it was observed that in some cases, this assumption overestimates the actual live load while underestimating it in others. Tarhini and Frederick [28] studied the influence of girder spacing on LLDF for concrete I-girder bridges and observed that the linearity correlation assumption is incorrect. Additionally, recent research has revealed that spacing between girders is not the sole factor influencing live load distribution; it has a major impact. Zokaie et al. [29] investigated the effect of span length on LLDF for concrete I-girder bridges and observed that interior girders consistently displayed more nonlinear behavior than outside girders throughout all span lengths. Tarhini and Frederick [28] also found a quadratic increase in the distribution factor when taking into account the increasing vehicle count with a longer span. Zokaie [30] investigated the impact of girder location on LLDF for concrete I-girder bridges and concluded that interior girders are less responsive to truck location than exterior girders.

Finally, no studies were carried out to evaluate LLDF for precast U-girder bridges. Furthermore, no studies were carried out to investigate the validity of AASHTO-LRFD equations for calculating LLDF. Therefore, it became necessary to conduct additional research on this kind of bridge girder.

3. Methodology

3.1. Overview of the study bridges

To investigate the main factors that influence the LLDF for precast U-girder bridges, a comprehensive parametric analysis was carried out using FEA. 52 prototype bridges were analyzed to evaluate the values of LLDF for outside and inside girders and study the effect of various parameters on those values. The prototype bridges' behavior was studied using the AASHTO-LRFD Specifications' live load model. The following criteria were used to select and model all of the studied bridges:

1. **Span length**

All bridges studied were assumed to have straight and simply supported spans, with span lengths of 15, 30, 45, and 60 meters.

2. **Deck width**

Various widths were chosen to accommodate two, three, four, and five-lane loading.

3. **Girder Spacing**

The distance between precast U-girders is assumed to be twice the upper width of the girder cross-section.

4. **Girder Depth**

Girder depth was determined as a function of span length (L) according to AASHTO-LRFD specifications, and it is 0.045 L.

5. Lane Width

The width of traffic lanes is calculated by dividing the curb-to-curb width by the number of lanes. It was assumed that the traffic lane was not to be less than 3.66 m.

6. Deck Slab

The thickness of the concrete slab is assumed to be 20cm, with full shear interaction with the precast U-girders.

Finally, the typical cross-section of the studied bridges are shown in Fig. 1. Table 1 illustrates Geometric properties of the prototype bridges used in the parametric study.

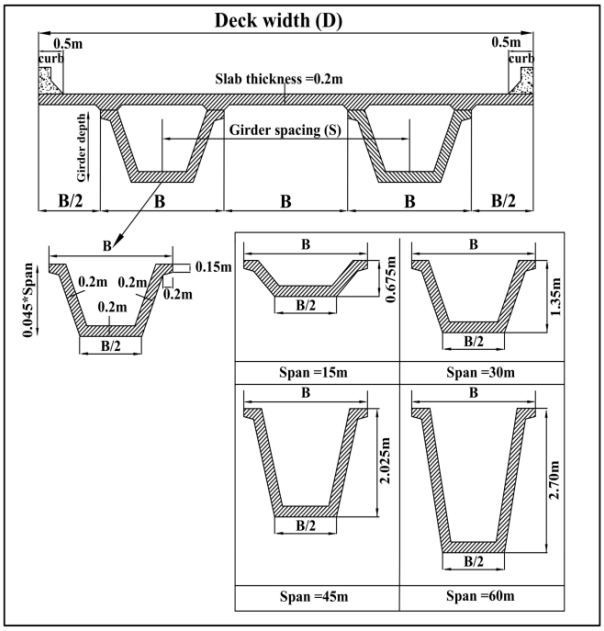

Fig. 1. Typical cross section for a prototype bridge.

3.2. Materials Properties

The characteristic compressive strength of reinforced concrete (F_{cu}) is assumed to be 40 N/mm^2. Table 2 summaries the different properties of the materials used in the design of selected bridges. Young's modulus was determined according to AASHTO-LRFD specifications by Equation (1).

$$E_C = 0.043\gamma_c^{1.5} [(0.76/0.97)* F_{cu}]^{0.5} \quad (1)$$

Where E_C is the elastic modulus of concrete (MPa), γ_c is the unit density of concrete (kg/m^3), F_{cu} is the compressive strength of concrete (MPa).

Table 1. Geometric properties of the prototype bridges used in the parametric study.

No. of Lanes	Span length (m)	No. of Girders	Girder spacing (m)	Deck Width (m)	Lane Width (m)
2	15	2	5	10	4.5
		3	3.34	10	4.5
		4	2.5	10	4.5
	30	2	5	10	4.5
		3	3.34	10	4.5
		4	2.5	10	4.5
	45	2	5	10	4.5
		3	3.34	10	4.5
		4	2.5	10	4.5
	60	2	5	10	4.5
		3	3.34	10	4.5
		4	2.5	10	4.5
3	15	2	6.5	13	4.5
		3	4.33	13	4.5
		4	3.25	13	4.5
	30	2	6.5	13	4.5
		3	4.33	13	4.5
		4	3.25	13	4.5
	45	2	6.5	13	4.5
		3	4.33	13	4.5
		4	3.25	13	4.5
	60	2	6.5	13	4.5
		3	4.33	13	4.5
		4	3.25	13	4.5
4	15	3	5.34	16	3.75
		4	4	16	3.75
		5	3.2	16	3.75
	30	3	5.34	16	3.75
		4	4	16	3.75
		5	3.2	16	3.75
	45	3	5.34	16	3.75
		4	4	16	3.75
		5	3.2	16	3.75
	60	3	5.34	16	3.75
		4	4	16	3.75
		5	3.2	16	3.75
5	15	3	6.5	19.5	3.7
		4	4.87	19.5	3.7
		5	3.9	19.5	3.7
		6	3.25	19.5	3.7
	30	3	6.5	19.5	3.7
		4	4.87	19.5	3.7
		5	3.9	19.5	3.7
		6	3.25	19.5	3.7
	45	3	6.5	19.5	3.7
		4	4.87	19.5	3.7
		5	3.9	19.5	3.7
		6	3.25	19.5	3.7
	60	3	6.5	19.5	3.7
		4	4.87	19.5	3.7
		5	3.9	19.5	3.7
		6	3.25	19.5	3.7

Table 2. Materials properties.

Properties	Value
Compressive Strength of Concrete (F_{cu})	40 N/mm^2
Density of concrete (γ_c)	25 KN/m^3
Elastic modulus of concrete (E_c)	30090 N/mm^2
Passion's ratio (υ)	0.20
coefficient of thermal expansion (α)	0.00001
Shear modulus (G)	9223 N/mm^2

3.3. Finite Element Modeling

The 3-D FE models for these bridges were created with CSI Bridge software. The precast U-girders, deck slab above the girders, and diaphragms were modelled using a three-dimensional shell element. Each shell element has four corner nodes and six degrees of freedom, including three displacements (U1, U2, and U3) and three rotations (φ1, φ2, and φ3). Because mesh density is crucial in FE modelling, coarse meshing around complicated regions may produce incorrect results [31]. Unrealistic mesh sizes are avoided during modelling by using a reduced mesh size (0.3m x 0.3m), as shown in Fig. 2. Geometric nonlinearity was not considered in this study. All of the studied bridges were considered to be straight and simply supported by a hinge at one end and a roller on the other. The concrete deck slab was considered to have complete shear interaction with the precast U-girders.

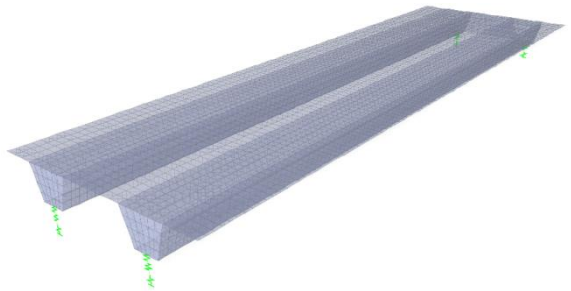

Fig. 2. FE model of a typical two U-girders bridge.

3.4. Design Live Loads According to AASHTO-LRFD Specifications

The designer engineer can use all of the exclusion vehicles listed in the Transportation Research Board database to simulate the serious impacts of live loads, but this work will be difficult and time-consuming [32]. As a result, the need for modeling live loads with a simple model is important. The AASHTO standard specification [33] created a model and called it the HS20-44 Model. Then, this model was developed and improved according to AASHTO-LRFD specifications and called the (HL-93) Model. The live loads in this model are truck loads, lane loads, and tandem loads. Figs. 3 and 4 illustrate the design truck and tandem configurations used in AASHTO-LRFD requirements. The design force that produces the largest live load effect is determined by the larger load of tandem with the load of the lane or the load of a truck (HL-93) with the load of the lane.

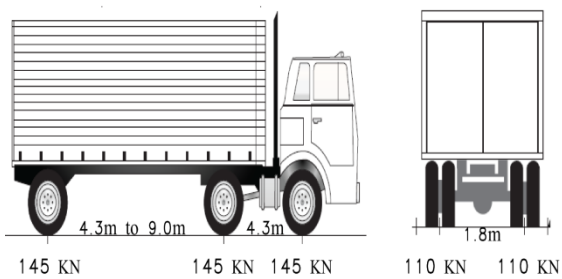

Fig. 3. Design truck load (AASHTO-LRFD Specifications).

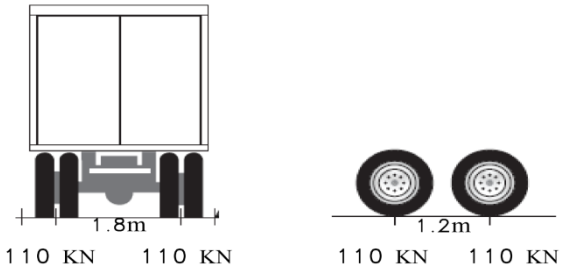

Fig. 4. Design tandem load (AASHTO-LRFD Specifications)

3.5. Calculation of LLDF for Girder (FEA)

The LLDF is calculated by dividing the three-dimensional straining action by the spine model straining action, as shown in Equation (2). The CSI Bridge program is used to create both the spine model and the 3-D model to calculate LLDF. The spine model is a frame element model for the bridge and represents the beam line model for the studied bridge, as shown in Fig. 5. The three-dimensional model of the studied bridge is shown in Fig. 6. Because all of the bridges studied in this research are simply supported, the maximum shear and moment distribution factors are found at the supports and midspan, respectively.

$$DF = F_{\text{3D model}} / F_{\text{Spine model}} \quad (2)$$

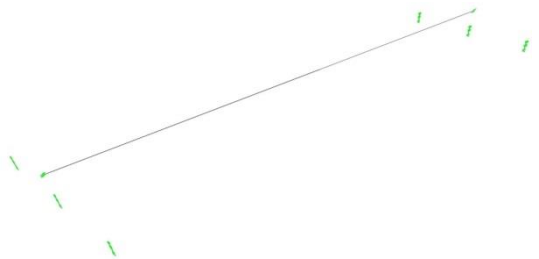

Fig. 5. Spine model for the studied bridge.

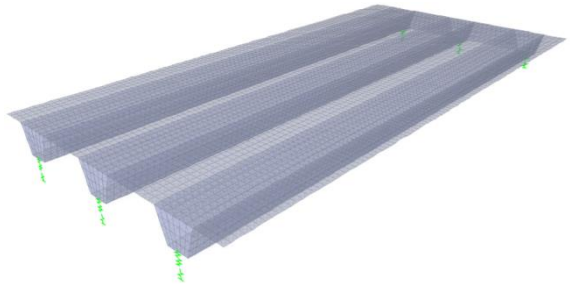

Fig. 6. Three-dimensional model for the studied bridge.

3.6. Calculation of LLDF for Girder (AASHTO Equations)

The moment distribution factor (MDF) can be determined according to AASHTO-LRFD Equations from Equations (3) to (5).

1. Interior Girder

$$MDF_{Int} = (S / 1900)^{0.6} * (S*d / L^2)^{0.125} \quad (3)$$

2. Exterior Girder

$$MDF_{Ext} = e * MDF_{Int} \quad (4)$$

$$e = 0.97 + (de / 8700) \quad (5)$$

Where S is the girders spacing (mm), d is the girder's depth (mm), L is the girder's span (mm), e is the correction factor for the exterior girder, and d_e is the gap between the inside edge of the curb and the web of the outside girder (mm).

The shear distribution factor (SDF) can be determined according to AASHTO-LRFD Equations from Equations (6) to (8).

1. Interior Girder

$$SDF_{Int} = (S / 2250)^{0.8} * (d / L)^{0.1} \quad (6)$$

2. Exterior Girder

$$SDF_{Ext} = e * SDF_{Int} \quad (7)$$

$$e = 0.8 + (d_e / 3050) \quad (8)$$

Where S is the girders spacing (mm), d is the girder's depth (mm), L is the girder's span (mm), e is the correction factor for the exterior girder, and d_e is the gap between the inside edge of the curb and the web of the outside girder (mm).

4. Results

4.1. Effect of each parameter on LLDF for inside and outside girders

The moment and shear distribution factor for each prototype bridge were determined using FEA. The impact of different parameters on LLDF was investigated as follows:-

4.1.1. Length of Girder

I. Moment distribution factor (MDF)

Figure 7 shows the impact of the girder's length on MDF for both outside and inside girders. MDF decreases as the girder's length increases, but at low rates for all prototype bridges, and the impact of changing the girder's length on MDF is smaller for outside girders than for inside girders.

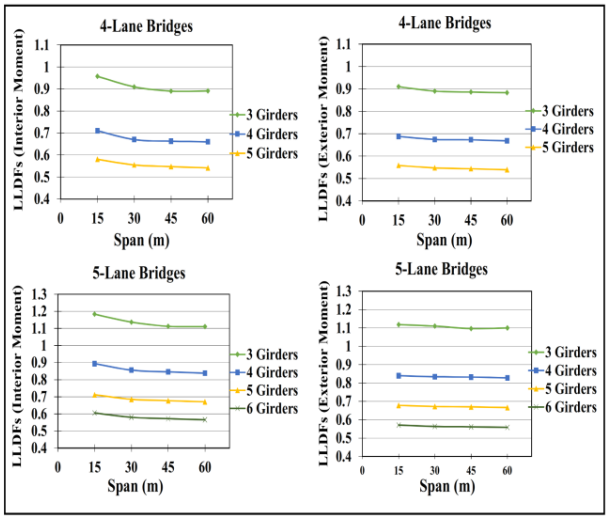

Fig. 7. Impact of girder's length on MDF.

II. Shear distribution factor (SDF)

Figure 8 shows the impact of the girder's length on SDF for both outside and inside girders. Unlike MDF, SDF increases as the girder's length increases for all prototype bridges, and the impact of changing the girder's length on SDF is higher for outside girders than for inside girders.

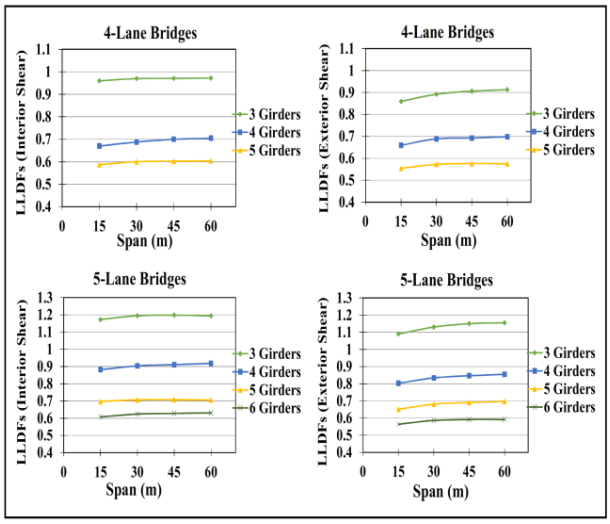

Fig. 8. Impact of girder's length on SDF.

4.1.2. Spacing of Girders

I. Moment distribution factor (MDF)

Girder spacing has an important impact on MDF, as shown in Fig. 9. When girder spacing is increased, MDF increases at nearly the same rate. As an illustrative example, for five-lane bridges with a 30m span, increasing the spacing from 3.25m to 6.50m (by 100%) causes an increase in the inside MDF from 0.57 to 1.13 (by 98%) and the outside MDF from 0.568 to 1.12 (by 97%).

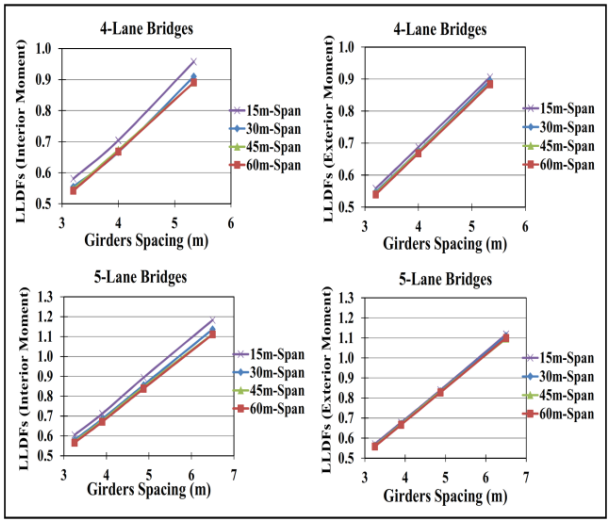

Fig. 9. Impact of girder spacing on MDF.

II. Shear distribution factor (SDF)

Much like MDF, girder spacing has an important impact on SDF, as shown in Fig. 10. When girder spacing is increased, SDF increases at nearly the same rate. As an illustrative example, for five-lane bridges with a 30m span, increasing the spacing from 3.25m to 6.50m (by 100%) causes an increase in the inside SDF from 0.61 to 1.19 (by 95%) and the outside SDF from 0.57 to 1.12 (by 96%).

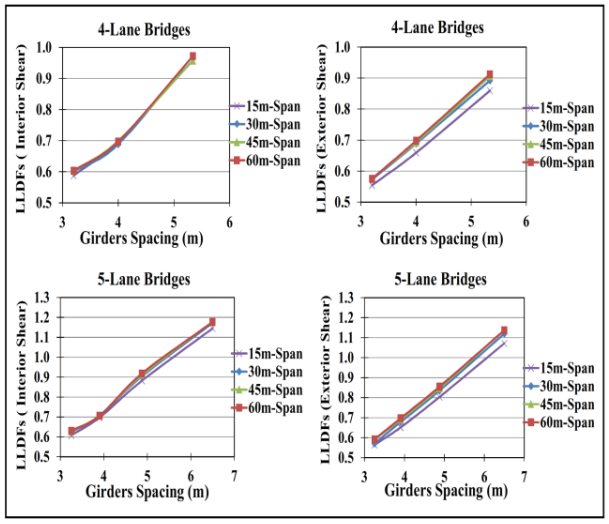

Fig. 10. Impact of girder spacing on SDF.

4.1.3. Number of Girders

I. Moment distribution factor (MDF)

The girder count has an important impact on MDF, as shown in Fig. 11. When the girder count is increased, MDF decreases at inverse rates with the girder count. As an illustrative example, for five-lane bridges with a 45-meter span, increasing the girder count from 3 to 6 (by 100%) causes a decrease in the inside MDF from 1.12 to 0.57 (by 49%) and the outside MDF from 1.1 to 0.56 (by 49%). This means that there is a linear relationship between the girder count and MDF. This behavior is consistent across all bridges, regardless of the girder's length.

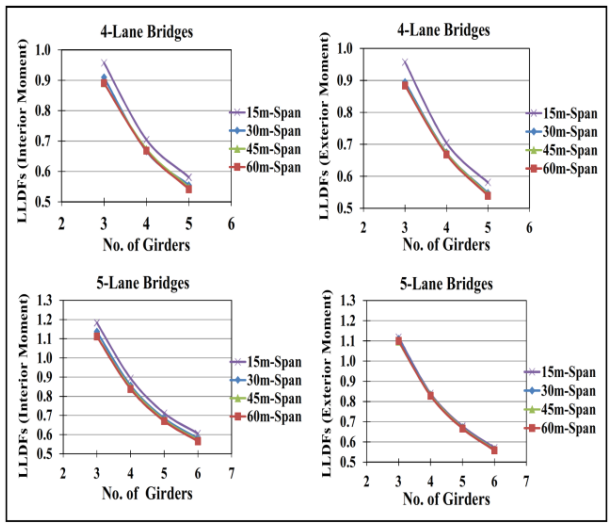

Fig. 11. Impact of girder count on MDF.

II. Shear distribution factor (SDF)

Much like MDF, the girder count has an important impact on SDF, as shown in Fig. 12. When the girder count is increased, SDF decreases at inverse rates with the girder count. As an illustrative example, for five-lane bridges with a 45-meter span, increasing the girder count from 3 to 6 (by 100%) causes a decrease in the inside SDF from 1.185 to 0.62 (by 48%) and the outside SDF from 1.13 to 0.58 (by 49%). Generally, the girder count is also inversely proportional to the SDF.

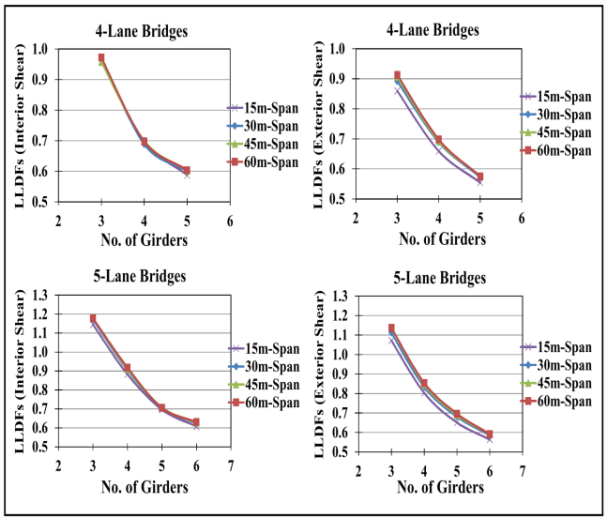

Fig. 12. Impact of girder count on SDF.

4.1.4. Number of Lanes

I. Moment distribution factor (MDF)

Lane count has an important impact on MDF, as shown in Fig. 13. MDF increases as the lane count increases from two to three, then plateaus as the lane count increases from three to four. As the lane count increases from four to five, MDF starts to increase again. This behavior is consistent regardless of the girder's length, for both inside and outside girders. This behavior is because each number of lanes is multiplied by a factor adopted by AASHTO-LRFD specifications, and the resultant is the net distributed load on the girders, as shown in Table 3. This factor was used to account for the rarity of fully loaded trucks crossing the structure side by side. Between three and four lanes, there is a very small difference in the total live load distributed on the girders. When comparing two and three lanes as well as four and five lanes, there is a large difference in the total live load distributed on the girders.

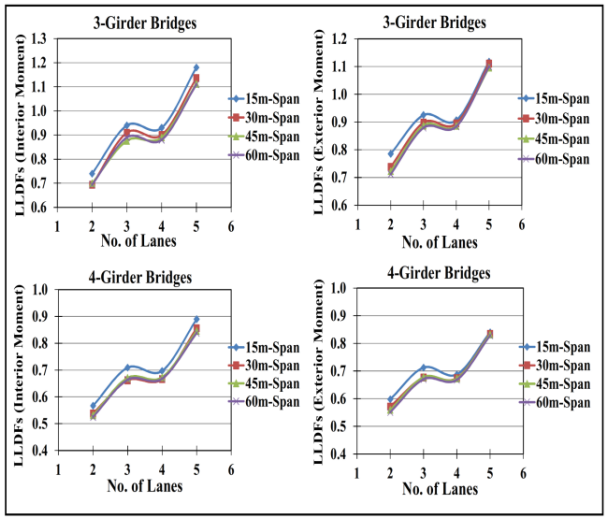

Fig. 13. Impact of lane count on MDF.

Table 3. Net distributed load on girders.

Number of Lanes	Factor	Distributed load on Girders
2	1	2
3	0.85	2.55
4	0.65	2.60
5	0.65	3.25

II. Shear distribution factor (SDF)

Figure 14 shows the impact of the lane count on SDF for both inside and outside girders. Much like MDF, the lane count has an important impact on SDF. SDF increases as the lane count increases from two to three, then plateaus as the lane count increases from three to four. As the lane count increases from four to five, SDF starts to increase again. This behavior is consistent regardless of the span length for both inside and outside girders. The explanation for this behavior is the same as for the MDF.

4.2. Comparison between calculating LLDF by AASHTO equations and FEA

The LLDF calculated using AASHTO equations is compared with those obtained from FEA. Scatter plots are used to compare these two sets of data. The calculated LLDF for a prototype bridge is represented by each point on the scatter plots. The line on the scatter plot is used to show the potential correlation between the results of the AASHTO-LRFD equations and FEA. The points above the line denote results from the AASHTO-LRFD equations that are overestimated. The

underestimated results of the AASHTO equations are indicated by the points that are below the line.

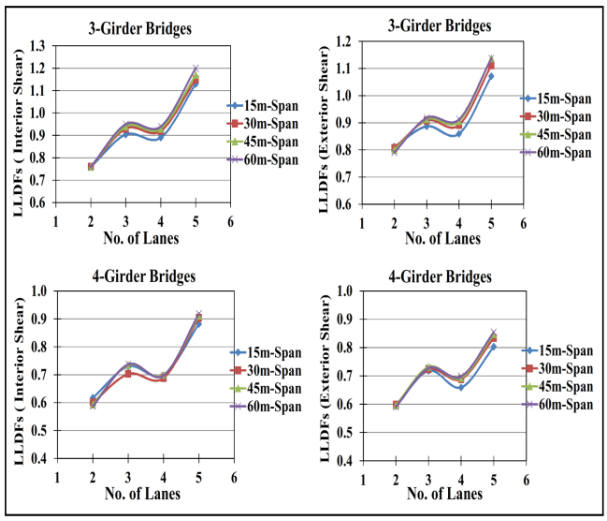

Fig. 14. Impact of lane count on SDF.

4.2.1. Comparison between calculating moment distribution factor by AASHTO equations and FEA

Moment distribution factors of the inside and outside girders are compared using the AASHTO-LRFD equations and FEA in Figs. 15 and 16. Based on these figures, the following notes can be summarized:

- For both inside and outside girders, the AASHTO-LRFD equations overestimate the MDF in many cases.
- In all of the prototype bridges, the rate of overestimation for the bridge reduces as the bridge length increases.
  In all of the prototype bridges, the rate of overestimation for the bridge increases with an increased lane count. Inside and outside girders indicate the same behavior.

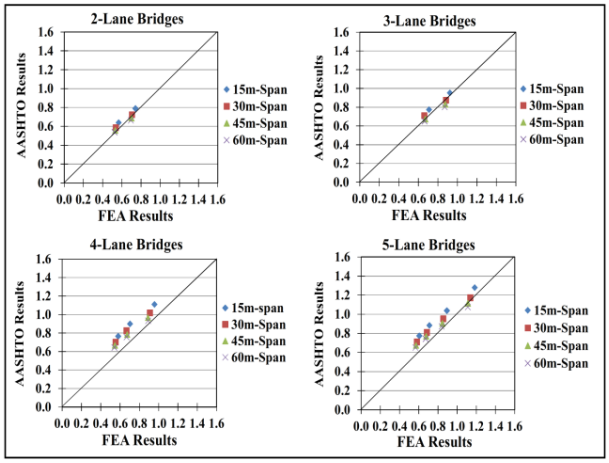

Fig. 15. Comparison of MDF for inside girders

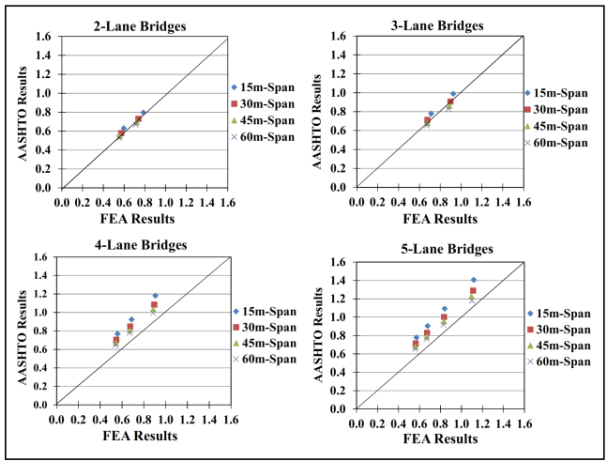

Fig. 16. Comparison of MDF for outside girders.

Figure 17 illustrates the difference between the AASHTO equations results to the FEA results. The following notes can be summarized based on this figure:

- The variation between the FEA and AASHTO equation values for the inside girders of 15-meter-span bridges ranges from 3.30% to 31.85%. For the outside girders, this variation varies from 1.50% to 37.50%.
- The variation between the FEA and AASHTO equation values for the inside girders of 30-meter-span bridges ranges from -1.20% to 26.60%. For the outside girders, this variation varies from -1.20% to 28.90%.
- The variation between the FEA and AASHTO equation values for the inside girders of 45-meter-span bridges ranges from -5.10% to 21.70%. For the outside girders, this variation varies from -4.00% to 23.40%.
  The variation between the FEA and AASHTO equation values for the inside girders of 60-meter-span bridges ranges from -8.00% to 18.90%. For the outside girders, this variation varies from -6.00% to 19.90%.

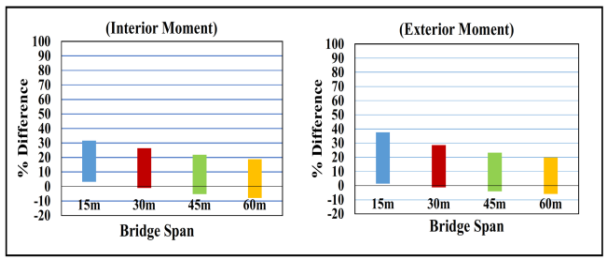

Fig. 17. Variation between AASHTO equations results to FEA results for calculating MDF.

4.2.2. Comparison between calculating shear distribution factor by AASHTO equations and FEA

Shear distribution factors of the inside and outside girders are compared using the AASHTO-LRFD equations and FEA in Figs. 18 and 19. Based on these figures, the following notes can be summarized:

- The AASHTO equations overestimate the SDF for all the bridges under study for both inside and outside girders.
- As bridge width increases, the rate of overestimation for bridges also increases. Two-lane bridges have the lowest overestimation value, while five-lane bridges have the highest value.
  Girder's length has little impact on the SDF.

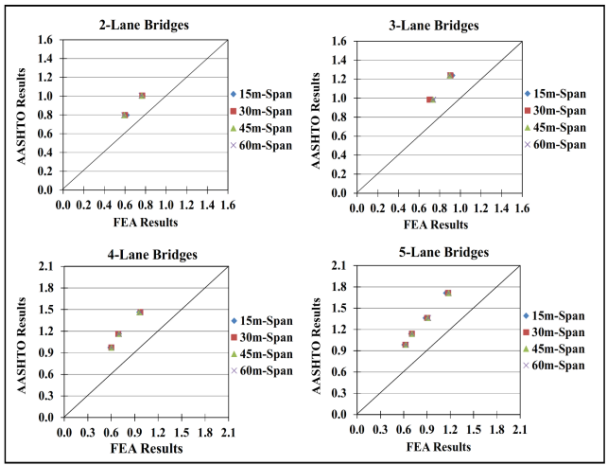

Fig. 18. Comparison of SDF for inside girders.

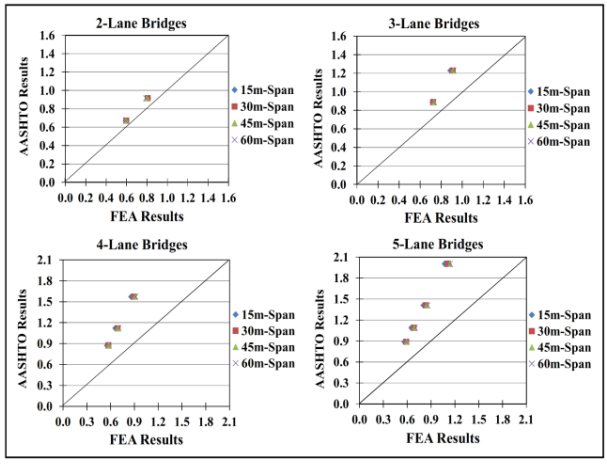

Fig. 19. Comparison of SDF for outside girders.

Figure 20 illustrates the difference between the AASHTO equations results to the FEA results. The following notes can be summarized based on this figure:

- The variation between the FEA and AASHTO equation values for the inside girders of 15-meter-span bridges ranges from 29.40% to 66.50%. For the outside girders, this variation varies from 12.75% to 87.00%.
- The variation between the FEA and AASHTO equation values for the inside girders of 30-meter-span bridges ranges from 31.00% to 68.90%. For the outside girders, this variation varies from 12.15% to 80.00%.
- The variation between the FEA and AASHTO equation values for the inside girders of 45-meter-span bridges ranges from 31.75% to 66.10%. For the outside girders, this variation varies from 12.60% to 76.00%.
- The variation between the FEA and AASHTO equation values for the inside girders of 60-meter-span bridges ranges from 32.50% to 66.60%. For the outside girders, this variation varies from 13.50% to 76.15%.

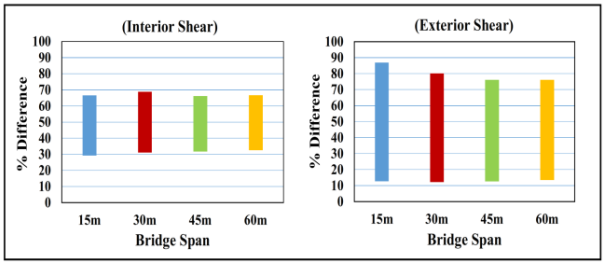

Fig. 20. Variation between AASHTO equations results to FEA results for calculating SDF.

5. Conclusion

According to the findings and parametric analysis of this study, it is possible to conclude:

- Girder's length has little impact on the LLDF because, with increasing girder's length, MDF slightly increases while SDF slightly decreases.
- Girder spacing has an important impact on MDF and SDF. When girder spacing is increased, the MDF and SDF increase at almost the same rates.
- Girder count has an important impact on MDF and SDF. When the girders count is increased, the MDF and SDF decrease at inverse rates to the girder count.

- Lane count has an important impact on MDF and SDF. MDF and SDF increase as the lane count increases from two to three, then plateaus as the lane count increases from three to four. As the lane count increases from four to five, the distribution factors start to increase again. This behavior is consistent regardless of the girder's length for both inside and outside girders. This behavior is because each number of lanes is multiplied by a factor adopted by AASHTO-LRFD specifications.
- In most cases, the AASHTO-LRFD equations overestimate both MDF and SDF. AASHTO equations for calculating the SDF offer a wider range of differences from the FEA results compared to equations for calculating the MDF.
- The accuracy of AASHTO-LRFD equations for MDF and SDF decreases as bridge width increases.
- The accuracy of AASHTO-LRFD equations for MDF decreases as the girder's length decreases.
- The use of AASHTO-LRFD equations to calculate SDF for wide bridges is uneconomic. The parametric study found that the maximum difference between AASHTO results to FEA results for five-lane bridges was 87%, while the maximum difference for two-lane bridges was 13.5%.

Further scope of research

It is suggested that further research efforts be directed towards the following:

1. Investigate the live load distribution factors for curved precast concrete U-girder bridges.
2. Investigate the live load distribution factors for precast concrete U-girder bridges of continuous span.
3. Study the effect of skewness on the values of live load distribution factors for precast U-girder bridges.

Notation List

E_c	Elastic modulus of concrete
γ_c	Unit density of concrete
F_{cu}	Compressive strength of concrete
υ	Passion's ratio
α	coefficient of thermal expansion
G	Shear modulus
S	Spacing of girder
d	Depth of girder
L	Span of girder
e	correction factor for the exterior girder
d_e	Gap between the inside edge of the curb and the web of the outside girder
AASHTO	American Association of State Highway and Transportation Officials
LRFD	Load and Resistance Factor Design
HL-93	Live load model according to AASHTO Load and Resistance Factor Design specification
HS20-44	Live load model according to AASHTO standard specification
SAP	Structural analysis program
CSI	Computers and structures, Inc.
FEA	Finite element analysis
LLDF	Live load distribution factor
DF	Distribution factor
SDF	Shear distribution factor
MDF	Moment distribution factor

Funding

The funder has played no role in the research.

Conflict of interest

The authors declare no competing interests.

Authors contribution statement

Kamel T. Kamel: Project administration, Writing-original draft, Validation, Conceptualization, Methodology.

Ahmed H. Amer: Investigation, Resources, Writing-review & editing, Conceptualization, Formal analysis.

Ahmed Z. Hanafi: Investigation, Formal analysis, Methodology.

References

[1] Furinghetti M, Pavese A, Lunghi F, Silvestri D. Strategies of structural health monitoring for bridges based on cloud computing. J Civ Struct Heal Monit 2019;9:607–16. https://doi.org/10.1007/s13349-019-00356-5.

[2] Bayraktar A, Altunişik AC, Türker T. Structural health assessment and restoration procedure of an old riveted steel arch bridge. Soil Dyn Earthq Eng 2016;83:148–61. https://doi.org/10.1016/j.soildyn.2016.01.012.

[3] Jang S, Li J, Spencer BF. Corrosion Estimation of a Historic Truss Bridge Using Model Updating. J Bridg Eng 2013;18:678–89. https://doi.org/10.1061/(asce)be.1943-5592.0000403.

[4] Bonopera M, Liao WC, Perceka W. Experimental–theoretical investigation of the short-term vibration response of uncracked prestressed concrete members under long-age conditions. Structures, vol. 35, Elsevier; 2022, p. 260–73. https://doi.org/10.1016/j.istruc.2021.10.093.

[5] Yang J, Guo T, Li A. Experimental investigation on long-term behavior of prestressed concrete beams under coupled effect of sustained load and corrosion. Adv Struct Eng 2020;23:2587–96. https://doi.org/10.1177/1369433220919067.

[6] Gocál J, Odrobiňák J. On the influence of corrosion on the load-carrying capacity of old riveted bridges. Materials (Basel) 2020;13. https://doi.org/10.3390/ma13030717.

[7] Ataei S, Miri A, Jahangiri M. Assessment of load carrying capacity enhancement of an open spandrel masonry arch bridge by dynamic load testing. Int J Archit Herit 2017;11:1086–100. https://doi.org/10.1080/15583058.2017.1317882.

[8] Wang X, Mao X, Frangopol DM, Dong Y, Wang H, Tao P, et al. Full-scale experimental and numerical investigation on the ductility, plastic redistribution, and redundancy of deteriorated concrete bridges. Eng Struct 2021;234:111930. https://doi.org/10.1016/j.engstruct.2021.111930.

[9] Olaszek P, Łagoda M, Casas JR. Diagnostic load testing and assessment of existing bridges: examples of application. Struct Infrastruct Eng 2014;10:834–42. https://doi.org/10.1080/15732479.2013.772212.

[10] Dong C, Bas S, Debees M, Alver N, Catbas FN. Bridge Load Testing for Identifying Live Load Distribution, Load Rating, Serviceability and Dynamic Response. Front Built Environ 2020;6:46. https://doi.org/10.3389/fbuil.2020.00046.

[11] Sun Z, Siringoringo DM, Fujino Y. Load-carrying capacity evaluation of girder bridge using moving vehicle. Eng Struct 2021;229. https://doi.org/10.1016/j.engstruct.2020.111645.

[12] Gatti M. Structural health monitoring of an operational bridge: A case study. Eng Struct 2019;195:200–9. https://doi.org/10.1016/j.engstruct.2019.05.102.

[13] Lee ZK, Bonopera M, Hsu CC, Lee BH, Yeh FY. Long-term deflection monitoring of a box girder bridge with an optical-fiber, liquid-level system. Structures, vol. 44, Elsevier; 2022, p. 904–19. https://doi.org/10.1016/j.istruc.2022.08.048.

[14] Harris DK. Assessment of flexural lateral load distribution methodologies for stringer bridges. Eng Struct 2010;32:3443–51. https://doi.org/10.1016/j.engstruct.2010.06.008.

[15] Seo J, Phares B, Wipf TJ. Lateral Live-Load Distribution Characteristics of Simply Supported Steel Girder Bridges Loaded with Implements of Husbandry. J Bridg Eng 2014;19:4013021. https://doi.org/10.1061/(asce)be.1943-5592.0000558.

[16] Ravazdezh F, Seok S, Haikal G, Ramirez JA. Effect of Nonstructural Elements on Lateral Load Distribution and Rating of Slab and T-Beam Bridges. J Bridg Eng 2021;26:4021063.

https://doi.org/10.1061/(asce)be.1943-5592.0001766.

[17] Hughs E, Idriss R. Live-Load Distribution Factors for Prestressed Concrete, Spread Box-Girder Bridge. J Bridg Eng 2006;11:573–81. https://doi.org/10.1061/(asce)1084-0702(2006)11:5(573).

[18] A Unified Approach for LRFD Live Load Moments in Bridge Decks by Christopher Higgins 1 , O. Tugrul Turan 2 , Robert J. Connor 3 , and Judy Liu 3 n.d.

[19] Specifications LBD. American Association of State Highway and Transportation Officials (AASHTO). Washington, DC, USA 2012.

[20] Alawneh M, Tadros M, Morcous G. Innovative System for Curved Precast Posttensioned Concrete I-Girder and U-Girder Bridges. J Bridg Eng 2016;21:4016076. https://doi.org/10.1061/(asce)be.1943-5592.0000938.

[21] Wu X, Li H. Experimental and analytical behavior of a prestressed U-shaped girder bridge. Struct Eng Mech 2017;61:427–36. https://doi.org/10.12989/sem.2017.61.3.427.

[22] SAP2000. Finite Element Analysis and Design of Structures 2004.

[23] CSI Bridge. Finite element analysis and design of bridges 2014.

[24] Tiwari S, Bhargava P. Load Distribution Factors for Composite Multicell Box Girder Bridges. J Inst Eng Ser A 2017;98:483–92. https://doi.org/10.1007/s40030-017-0243-x.

[25] Terzioglu T, Hueste MBD, Mander JB. Live Load Distribution Factors for Spread Slab Beam Bridges. J Bridg Eng 2017;22:4017067. https://doi.org/10.1061/(asce)be.1943-5592.0001100.

[26] Thakuria P, Talukdar S. Live Load Distribution Factor in Precast I-Girder Bridge. IOP Conf Ser Mater Sci Eng 2018;431. https://doi.org/10.1088/1757-899X/431/11/112012.

[27] Razzaq MK, Sennah K, Ghrib F. Live load distribution factors for simply-supported composite steel I-girder bridges. J Constr Steel Res 2021;181:106612. https://doi.org/10.1016/j.jcsr.2021.106612.

[28] Tarhini KM, Frederick GR. Wheel Load Distribution in I-Girder Highway Bridges. J Struct Eng 1992;118:1285–94. https://doi.org/10.1061/(asce)0733-9445(1992)118:5(1285).

[29] Zokaie T, Imbsen RA, Osterkamp TA. Distribution of wheel loads on highway bridges. Transp Res Rec 1991;1290:119–26.

[30] Zokaie T. AASHTO-LRFD Live Load Distribution Specifications. J Bridg Eng 2000;5:131–8.

[31] Quadri AI, Ali K. Numerical Appraisal of Reinforced Concrete Dapped-End Girder Under High-Fatigue Fixed Pulsating and Moving Loads. Transp Res Rec 2024;2678:257–78. https://doi.org/10.1177/03611981231184176.

[32] Manual HC. Transportation Research Board of the National Academies. Washington, DC: 2010.

[33] AASHTO. “Standard Specifications for Highway Bridges American Association of State Highway and Transportation Officials”, ABD. 2002.